Toughening mechanisms in bioinspired multilayered materials

Askarinejad, Sina; Rahbar, Nima

Published in:
Journal of the Royal Society. Interface

DOI:
10.1098/rsif.2014.0855

Publication date:
2015

INTERFACE

rsif.royalsocietypublishing.org

Research

Cite this article: Askarinejad S, Rahbar N. 2015 Toughening mechanisms in bioinspired multilayered materials. *J. R. Soc. Interface* **12**: 20140855.
http://dx.doi.org/10.1098/rsif.2014.0855

Received: 31 July 2014
Accepted: 29 October 2014

Subject Areas:
biomimetics

Keywords:
bioinspired materials, multilayered, toughening mechanism, biological composites, abalone nacre

Author for correspondence:
Nima Rahbar
e-mail: nrahbar@wpi.edu

THE ROYAL SOCIETY
PUBLISHING

Toughening mechanisms in bioinspired multilayered materials

Sina Askarinejad[1] and Nima Rahbar[1,2]

[1]Department of Mechanical Engineering, and [2]Department of Civil and Environmental Engineering, Worcester Polytechnic Institute, Worcester, MA, USA

Outstanding mechanical properties of biological multilayered materials are strongly influenced by nanoscale features in their structure. In this study, mechanical behaviour and toughening mechanisms of abalone nacre-inspired multilayered materials are explored. In nacre's structure, the organic matrix, pillars and the roughness of the aragonite platelets play important roles in its overall mechanical performance. A micromechanical model for multilayered biological materials is proposed to simulate their mechanical deformation and toughening mechanisms. The fundamental hypothesis of the model is the inclusion of nanoscale pillars with near theoretical strength ($\sigma_{th} \sim E/30$). It is also assumed that pillars and asperities confine the organic matrix to the proximity of the platelets, and, hence, increase their stiffness, since it has been previously shown that the organic matrix behaves more stiffly in the proximity of mineral platelets. The modelling results are in excellent agreement with the available experimental data for abalone nacre. The results demonstrate that the aragonite platelets, pillars and organic matrix synergistically affect the stiffness of nacre, and the pillars significantly contribute to the mechanical performance of nacre. It is also shown that the roughness induced interactions between the organic matrix and aragonite platelet, represented in the model by asperity elements, play a key role in strength and toughness of abalone nacre. The highly nonlinear behaviour of the proposed multilayered material is the result of distributed deformation in the nacre-like structure due to the existence of nano-asperities and nanopillars with near theoretical strength. Finally, tensile toughness is studied as a function of the components in the microstructure of nacre.

1. Introduction

Learning lessons from nature is a key element in the design of tough and strong composites. Many biological materials are composites with outstanding mechanical properties, while the microstructural components from which they are made do not possess similar properties. Nacre is a wonder of nature in its mechanical properties in terms of strength and toughness. This structural material exhibits a toughness (in energy terms) some orders of magnitude higher than that of its primary component ($CaCO_3$), and its strength is among the highest in shell structures [1–3]. Inspired by this structure, there have been significant efforts in the past decades to synthesize new materials with mechanical performance comparable to nacre in the past decades [4–15]. The essence of success is to understand the deformation mechanisms inherent in nacre. Hence, mechanical models are needed in order to answer these fundamental questions. The main goal of this study is to explain the basic deformation and toughening mechanisms and the resulting stress distribution in nacre-like multilayered materials through different stages of deformation.

Nacre is a natural composite made of 95% brittle aragonite platelets ($CaCO_3$ tablet) [16] and only 5% biological macromolecules; this has an important effect on nacre's fracture resistance [17]. The elastic modulus of the aragonite is generally assumed to be about $E = 100$ GPa [1,18]. A relatively thick (0.2–0.9 μm) and brittle aragonite is separated by nanoscale inter-layers (approx. 20 nm). The mineral layer

exists as closely packed polygonal tablets (3–5 μm diameters), separated by a nanoscale organic gap. The tensile strength and Young's modulus of wet nacre are reported to be approximately 140 MPa and 70 GPa, respectively [1,19,20]. The existence and role of water in the structure of nacre has been investigated by many researchers. It has been mentioned that the effect of water was to increase the ductility of nacre and increase the toughness by almost 10-fold [21,22].

Wang *et al.* [23] performed a study investigating the behaviour of abalone nacre and pearl oyster nacre under different test set-ups. The results of four-point bending tests show a Young's modulus of $E \sim 70$ GPa. The tensile curves are highly nonlinear and the yield stress is in the range of 105–140 MPa [23]. Other researchers have described the origin of toughness by crack deflection, fibre pull-out and organic matrix bridging [9,24]. Barthelat *et al.* [25,26] also performed a numerical and experimental investigation on deformation and fracture of nacre and proposed their results from image correlation, finding the experimental crack resistance curves for nacre with logarithmic function fit [25]. They claimed that the large breaking strain in the experiments and simulations was due to the waviness of the platelets. However, the numerical model based on the waviness of the platelets over-predicts the strength and under-predicts the ductility [26]. Li *et al.* [27] studied the nanoscale structure of red abalone shell and suggested that the tablets themselves are made of nanograins [27]. They found that although the tablet strength does not directly affect the deformation mechanism, the integrity of the tablets is due to these nanograins, which prevent the tablets from breaking during the deformation process. Nanoindentation was used by other research groups to study the properties of the individual components of nacre [28]. These studies emphasize that the platelets possess a high fracture stress, i.e. they will remain intact in the deformation process of nacre under low strain rates.

Many researchers believe that the organic matrix in the structure of nacre plays the key role in its high fracture toughness [17]. There has therefore been great interest in understanding the mechanical behaviour of the organic matrix. Smith *et al.* [29] believe that the natural adhesives elongate in a stepwise manner. They claimed that opening of the organic macromolecules' folded domains cause a modular elongation and is the origin of toughness in the natural fibres and adhesives. In that study, a single molecule of protein was pulled, and the behaviour of a short molecule and long molecule was investigated. It was mentioned that the short molecules behave more stiffly but required less energy to break [29]. In another study, Mohanty *et al.* [7] investigated the mechanical response of the organic matrix of nacre. Atomic force microscopy (AFM) was used to pull the organic phase away from the aragonite. The results show a high adhesion force between the proteins and the platelets and are evidence of organic–inorganic interactions [7]. Different experimental approaches have been used to determine the mechanical properties of the organic matrix in different stages of deformation [30–34].

Molecular dynamics simulations have also been used to investigate the role of the organic matrix on the mechanical response of nacre [35]. In that study, by Ghosh *et al.* [35], the mechanical response of the organic matrix in proximity of aragonite platelets was investigated and it was indicated that the high elastic modulus of the proteins may be due to the mineral–organic interactions. Barthelat *et al.* [26] used a two-dimensional finite-element model of indentation to fit the experimental nano-indentation load–penetration depth curves of nacre, giving an elastic modulus of around 2.84 GPa [26]. Xu *et al.* [32] considered the extension of a single biopolymer molecule as a series of helical springs, so that unfolding of one module increases the stiffness of the biopolymer molecule. In that study, it was shown that a larger spring outer diameter causes a smaller spring constant [36]. Overall, these studies showed that the organic matrix has a high elastic modulus in the range of 4.0 GPa, while unfolding the entangled domains increases its stiffness during the deformation process.

Schaffer *et al.* [37] claimed that abalone nacre forms by growth through mineral bridges rather than on heteroepitaxial nucleation [37], and many researchers have confirmed this [38–40]. Song *et al.* [41] were the first to consider the role of pillars (mineral bridges) in enhancing the strength of the structure [41]. They believe that the mineral bridges between the tablets increase the fracture strength of the organic matrix interface by a factor of 5. It was also shown that the cracks propagate along the organic matrix. Their transmission electron microscopy images showed that the average length of the cracks in each of the organic layers is about 2 μm, and this is because of the crack deflection due to the presence of mineral bridges in the biomaterial. In another study, Song *et al.* [42] studied the properties and performance of the organic matrix and mineral bridges in nacre's structure [42]. In that study, it was shown that the microstructure of nacre should be referred to as 'brick–bridge–mortar' structure. Cartwright *et al.* [43] also studied the dynamics of nacre self-assembly which indicates the presence of the shear mineral bridges between the platelets in the nacre of gastropods [43]. Their observations show that the mineral tablets start growing through pores in the membrane and initiate the tablet above. They also pointed out how the pore size may influence the rate of growth of mineral bridges (incomplete growth will create asperities on the surface of the platelets). Similar crystalline orientation of platelets in different layers has been shown as strong evidence of the existence of mineral bridges and of a self-assembly mechanism in nacre [44–46]. Checa *et al.* [47] also used high-resolution imaging techniques to prove the existence of shear mineral bridges and asperities between the layers of platelets in the nacre of gastropods [47]. Furthermore, as Ghosh *et al.* [35] pointed out, the organic matrix behaves more stiffly in proximity of the minerals [35]. Hence, existence of pillars and asperities affect the mechanical properties of nacre through two mechanisms: (i) directly, by inclusion of their own properties and (ii) indirectly, by stiffening the organic matrix.

Beside experimentations and observations, there are different numerical and theoretical approaches to model the mechanical response of nacre [48–54]. Katti *et al.* [52] numerically modelled the mechanical behaviour of nacre with an elastic three-dimensional finite-element model based on a brick and mortar microstructure, assuming the organic matrix behaves linearly [55,56]. The results show that the organic layer needs to have a high modulus in order to capture the experimental results on nacre. Evans *et al.* [57] constructed a model consisting of platelets and asperities with a frictionless interface [57]. Their results show that the nanoscale asperities provide a strain-hardening large enough to ensure the formation of multiple dilatation bands but not so large that platelets fracture internally. Shao *et al.* [58] also studied the size effect on the mechanical response of

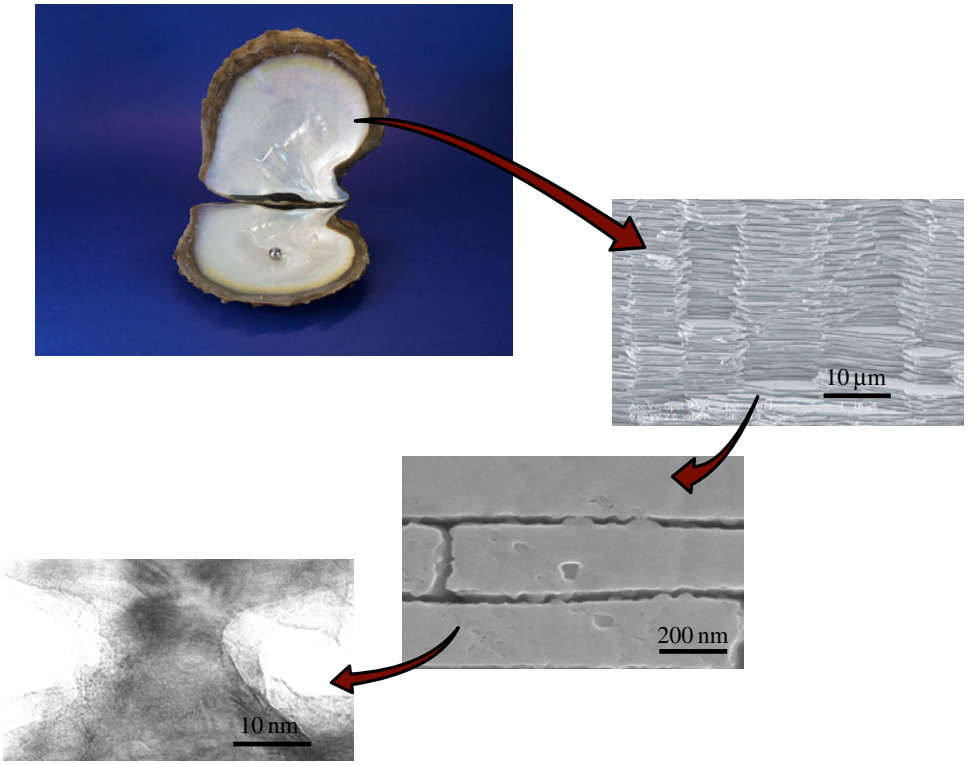

Figure 1. Scanning electron microscopy (SEM) images of the microstructure of nacre [23]. (Online version in colour.)

nacre and proposed a discontinuous crack-bridging model for fracture toughness analysis of nacre [58]. The effect of pre-existing structural defects was investigated in the crack-bridging based model in another study by Shao *et al.* [59]. More recently, Begley *et al.* [60] studied the brick and mortar structure and proposed a model to guide the development of these composites. In that study, the uniaxial response of the brick and mortar composites was analysed and the role of different parameters such as the bricks' aspect ratio and the volume percentage of the mortar part were investigated. The proposed analytical model by Begley *et al.* [60] is used here to validate some of the results.

In this study, we show the role of platelets, mineral bridges (pillars), nanoscale asperities and the organic matrix in the overall deformation mechanism of nacre. The main and new hypotheses in our numerical model are that (i) the nanoscale pillars have near theoretical strength and (ii) the existence of these nanoscale features confine the organic matrix to the proximity of mineral platelets and hence, increase their otherwise low stiffness.

2. The micromechanical model

2.1. Nacreous structure

A detailed investigation on the microstructure of nacre reveals that the structure of abalone nacre is more than a mortar–brick repeating unit as shown in the increasing scale image, figure 1. Nano-asperities, proteins (organic matrix) and mineral pillars (previously referred to as mineral bridges) fill inside the inter-layers and gaps. The statistical studies on abalone nacre illustrate that the average length of one platelet on the cross section is approximately equal to 4.0 µm, and the aspect ratio of the platelets are generally around 8.0 [42] measured as L/D, where L is the length of the platelets and D is the thickness. The pillars are placed in the gap between two layers, normal to the longitudinal side of the platelets.

2.2. Finite-element models

Aragonite platelets were modelled as beam elements with a bending stiffness set to represent the flexural behaviour of hexagonal platelets with $E_{tab} = 100$ GPa, although they carry minimal bending stresses. The length of a single platelet was considered to be about 4.0 µm and its thickness was estimated to be about 0.52 µm. The inter-layer gap was 24 nm and the gap between two adjacent platelets in a layer was estimated as 20 nm. The density of the platelets was set to be around 3 gr cm^{-3}. The ABAQUS/Explicit software package was used to carry out the finite-element simulations.

The fundamental assumption in this model is that the strength of mineral bridges is equal to their *theoretical strength* $= \sigma \sim E/30$, since the gaps between the platelets are less than the critical length scale (30 nm) [51]. Hence pillars were modelled as link elements with stiffness equal to the shear modulus of aragonite $E_{pillars} = G_{tab} = 40.0$ GPa and $\sigma_{pillars} = 3.3$ GPa. The area fraction of pillars, β_1, was estimated to be about 1.0–4.0%. Moreover, since the density of the pillars in the central region of the platelets is higher than the density of pillars in the outer region of platelets [42], in our model, the pillars were modelled as link elements connecting the middle of the platelets in two adjacent rows in each unit-cell (figure 2).

In the proposed model, the behaviour of proteins is approximated to be linear elastic before failure. We believe that pillars and asperities confine the organic layer in between the aragonite platelets. This results in a high stiffness value for the organic matrix in the range of approximately 4.0 GPa. The organic matrix's strength is considered to be near theoretical strength of approximately 200 MPa. The organic matrices in between the two neighbouring platelets

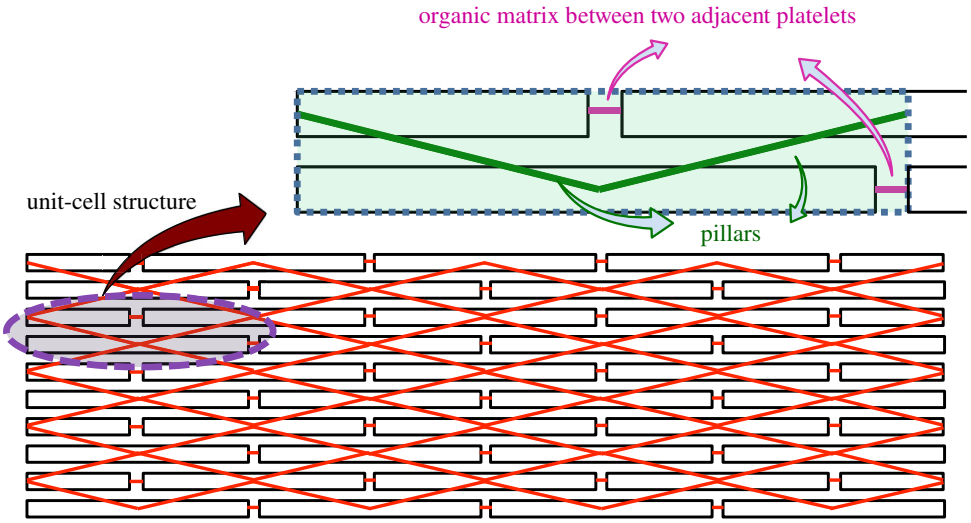

Figure 2. Schematic of the arrangement of the link elements representing the organic matrix, pillars and asperities in the model. (Online version in colour.)

were modelled as link elements connecting the edges of the platelets (figure 2).

It has been previously shown that the asperities in different layers interpose in many spots. This interlocking affects nacre's behaviour by involving more short molecules and making the organic matrix behave [56]. The nano-asperities in between two adjacent platelets provides confinement and entanglement of short molecules in the organic matrix in the proximity of mineral platelets. This is the physical mechanism that provides the high stiffness of the organic matrix. Observations also show nanoscale mineral islands are about 30–100 nm in diameter and 10 nm in amplitude. Nano-asperities show a statistical distribution with average spacing of 60–120 nm. [23]. Accordingly, the area fraction of the asperities, β_2, was estimated to be about 40.0%. Hence, the asperities were modelled as link elements to reflect the effects of the interactions of the organic matrix with platelets. This element fails when the displacement between the two platelets in adjacent layers reaches to the point of no interaction between the organic matrix and the platelet, which is when the stress in the organic matrix reaches its strength limit. The asperities are modelled as link elements with stiffness equal to the shear modulus of the organic matrix, $E_{\text{asperities}} =$ 1.6 GPa, and a strength of about 200 MPa.

The mechanical behaviour of each element in the structure of nacre is shown in figure 3. Using the material properties, geometry and area fraction of the components, a unit-cell model was created. Displacement was applied in equal time steps to the right-hand side of the system, while the left-hand side of the unit-cell was fixed in the *X*-direction. Figure 2 shows a schematic of the unit-cell structure and the way the link elements are arranged to capture the mechanical response of the proposed components. In this system, each element is guaranteed to behave in its natural state, e.g. pillars are modelled as link elements in the direction parallel to the platelets, which translates into shear behaviour with no bending.

The unit-cell was used to model the deformation mechanism in a super-cell representing the multilayered structure of nacre. The super-cell was composed of 10 elements in 20 layers for each simulation. Using symmetry, only a quarter of the sample was modelled under a four-point bending experiment. The four-point bending experiment was modelled by applying the linear displacement on the right-hand side of the super-cell as shown in figure 4. For a super-cell,

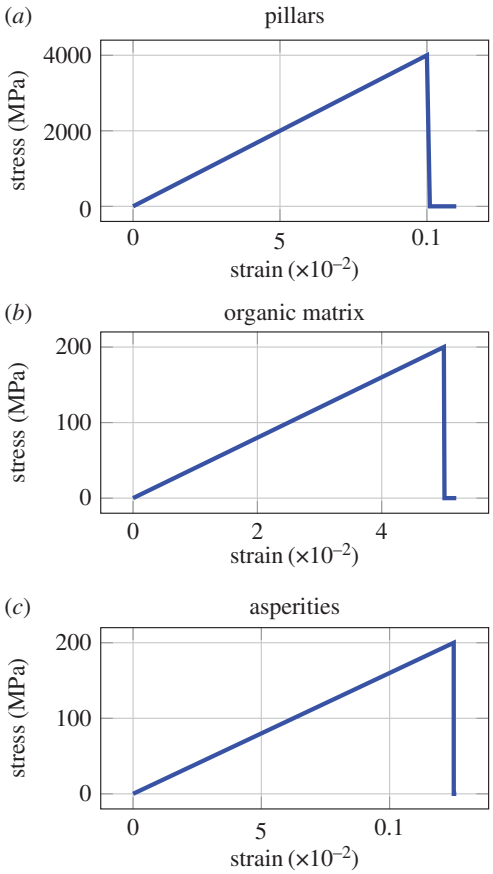

Figure 3. Stress–strain behaviour of the components present in the unit-cell: (*a*) pillars, (*b*) organic matrix and (*c*) asperities. (Online version in colour.)

average stress in the layers is plotted versus the average strain of the total cross section. The simulations were performed for several multilayered models, using the mechanical properties and the prescribed area fractions.

3. Results

3.1. Unit-cell behaviour and nacre micromechanical model

The simulation result for the mechanical behaviour of the unit-cell is presented in figure 5*a*. The structural components

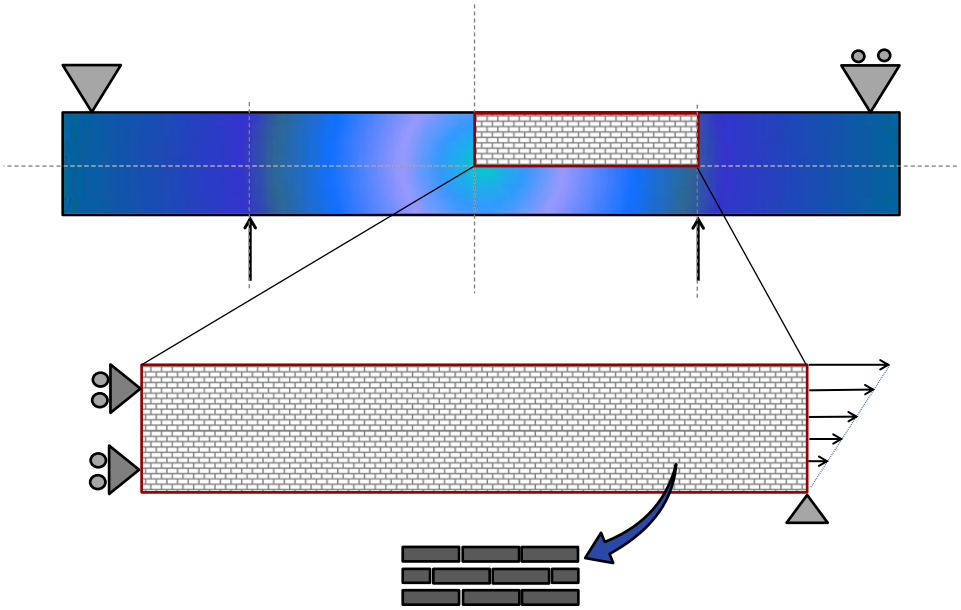

Figure 4. Schematic of model used for the simulation of the four-point bend experiment. (Online version in colour.)

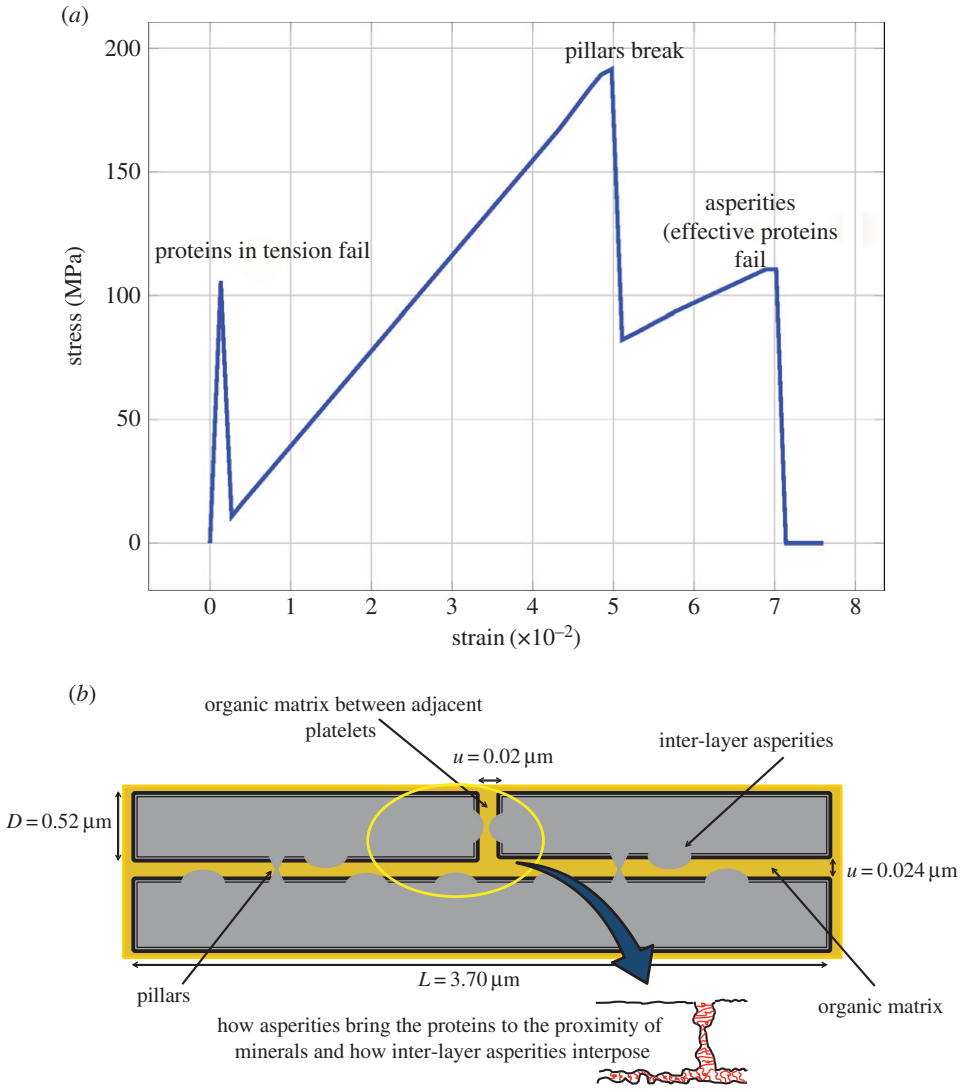

Figure 5. (*a*) Stress–strain plot of the suggested unit-cell and (*b*) schematic graph of components in the unit-cell structure. (Online version in colour.)

in the unit-cell are schematically presented in figure 5*b*. All elements carry the load during the early stages of deformation until the stress in the organic matrix under tension in both layers exceeds their strength. Hence, all the elements synergistically contribute to Young's modulus of the suggested unit-cell. The initial stiffness of the unit-cell with an organic matrix with stiffness value of 4.0 GPa, 40.0% area fraction of asperities and 2.0% of pillars is about

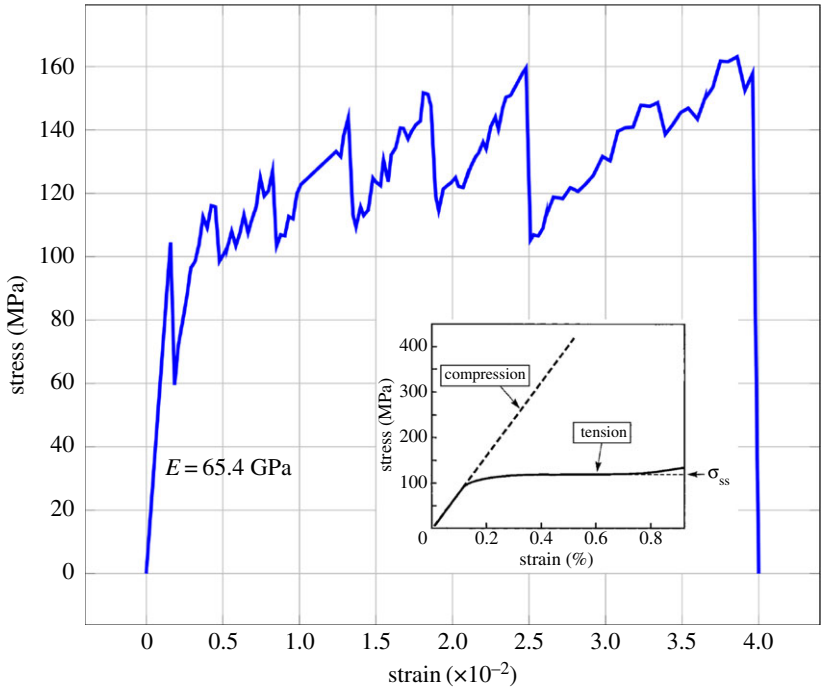

Figure 6. Nacre micromechanical model response (compared with the experimental results investigated by Evans *et al.* [57]). (Online version in colour.)

$E = 78.8$ GPa. In the second stage of the loading phase, the pillars and the proteins in shear carry the load. At the end of this stage, pillars break as the stress reaches their strength, and the proteins are the only elements that carry the load. In the third stage, the stiffness of the system comes from asperities (effective organic matrix). The simulation ends with the failure of the asperity elements, which represents the point of no organic–inorganic interaction between the proteins and the platelets due to the excessive displacement between the two parallel platelets with respect to each other.

The simulation result for a multilayered system similar to the microstructure of nacre is presented in figure 6. Here, average stress in the layers is plotted versus the average strain. Stress averaging is done by dividing the summation of the forces in each layer by the total cross-sectional area in every stage of deformation. The stress–strain curves are in agreement with the previous experimental results [57]. The experimental response of the four-point bending test on nacre showed a stiffness of about 70 GPa and a large inelastic deformation area in the stress–strain curve. These values are similar to the simulation results for a model with 40.0% area fraction of asperities, 2.0% area fraction of pillars and an organic matrix with stiffness of about 4.0 GPa. Additionally, the yield stress of 110 MPa and ultimate strength of 150 MPa is close to the experimental results of 105 MPa and 140 MPa, respectively. Progressive failures of the organic matrices, pillars and asperities make the model exhibit significant tensile toughness[1] and a large inelastic deformation. In nacre, tablet sliding spreads throughout the material, and each of the local extensions generated at local sliding zones add up and cause high strains measured at the macro-scale.

3.2. Toughening mechanism and the role of the components

In order to understand the effects of the platelets' aspect ratio on the overall mechanical properties of the multilayered

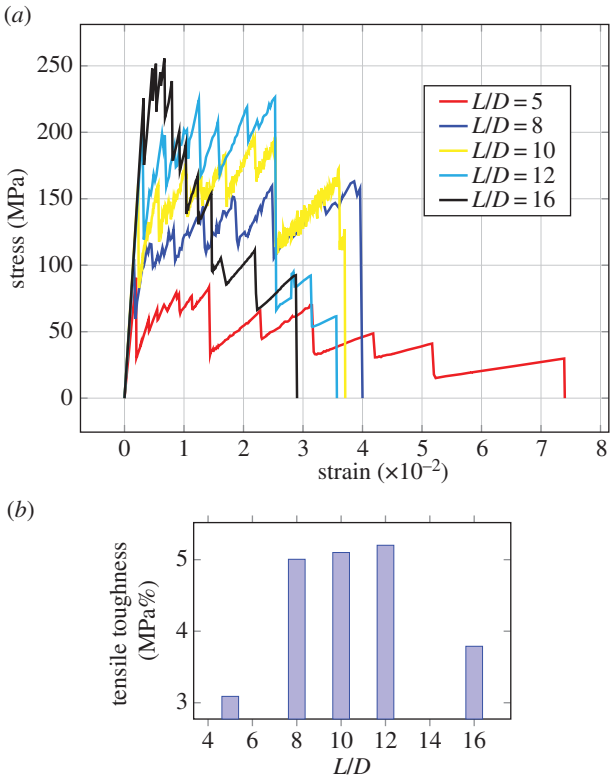

Figure 7. (*a*) Stress–strain plots for different aspect ratios of platelets, L/D, for $E_m = 4.0$ GPa, (*b*) Tensile toughness for different models as a function of the aspect ratio. (Online version in colour.)

system, additional micromechanical models were created for a constant area fraction of 40.0% asperities and 2.0% pillars. Two of these aspect ratios ($L/D = 5.0$, 6.0) are less than the aspect ratio of platelets in the nacre-like model and three of them ($L/D = 10.0$, 12.0, 16.0) are greater than that of nacre. The results of the models with platelets' aspect ratio of 5.0, 8.0, 10.0, 12.0 and 16.0 are presented in figure 7*a*. In all of these models, the thickness of the platelets is considered to

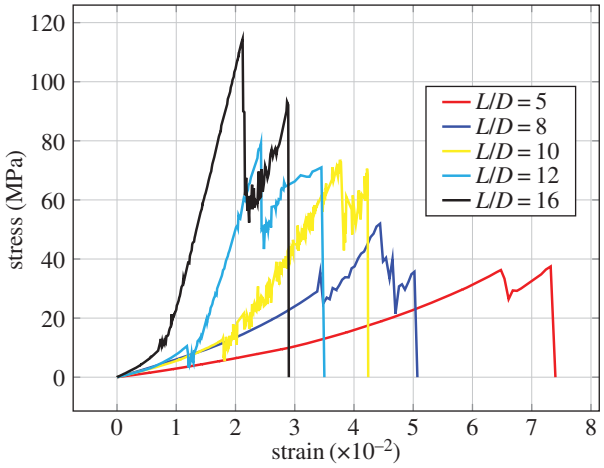

Figure 8. Stress–strain curves for models consisting of only pillars and asperities and different aspect ratios of platelets. (Online version in colour.)

be more than tens of nanometres and less than a micrometre. This is consistent with the optimal range of the platelets' aspect ratio to achieve higher fracture toughness, found by Shao *et al.* [58].

The results show that an increase in the platelets' aspect ratio results in a higher stiffness. The ultimate strength of the models also increase with an increase in the platelets' aspect ratio. However, it should be noted that aspect ratios that are higher than 12.0 do not result in an increase in the tensile toughness. Rabiei *et al.* [61] have also shown that the *pen shell* has low fracture toughness due to its high platelets' aspect ratio [61]. Figure 7*b* suggests that an aspect ratio around 12.0 is an optimal ratio for the design of these multilayered materials with nanoscale features.

The effects of the organic matrix on tension in the mechanical response of the models are studied by modelling multilayered systems consisting of only pillars and asperities. The stress–strain plots of these models are presented in figure 8. The material behaviour in this case is entirely nonlinear. Although all models have a low initial stiffness, their stiffness increases with an increase in deformation. Following this hardening behaviour, all models show a peak, followed by a significant drop in stress. While each fluctuation in the graph demonstrates the failure of a pillar or asperity element, the two significant drops in the stress–strain curve represent the failure of a series of elements together. This is followed by another hardening stage before the final failure. The initial stiffness and the ultimate strength also increases with an increase in the platelets' aspect ratio. However, the tensile toughness in these set of models is not affected by the aspect ratio.

The absolute value of the tensile toughness for the model with all components is higher than the tensile toughness for the model consisting of only pillars and asperities. However, this is purely related to the extra strain energy needed for the fracture of the organic matrix in between the two adjacent platelet in a row. These results also agree well with the experimental results on the samples of nacre with the organic matrix removed [62]. In that study, the calcination thermal treatment was used to remove the organic phase from the shell structure. Their results also show a significant drop in the stiffness and stress at break for these samples in comparison to the wet samples.

The unique deformation mechanism of the multilayered natural composite causes a distributed stress in all the components of the multilayered material, which creates high tensile toughness and large inelastic deformation. Figures 9 and 10 show stress distributions in the models with all elements and the models consisting of only pillars and asperities, respectively. The blue elements carry little or no force. Figure 9 demonstrates how failure propagates in the model and how stress distributes in the system until the last elements break, leading to failure of the system. Figure 10 illustrates the same process in the sample consisting of only pillars and asperities. In this model, the deformation is evenly and symmetrically distributed throughout the system. The stress contours clearly demonstrate that the deformation is distributed through a large portion of the model and the stress concentration is removed from the multilayered material system. This mechanism causes a strong and tough mechanical response. This fact is also indicated by other researchers [23,63]. Here, we emphasize that this mechanism in nacre is created by the existence of pillars and asperities which enhance the interaction between the organic matrix and the surface of the aragonite platelets.

The stress–strain curves for multilayered materials with a platelet aspect ratio of 16.0 and different values of organic matrix stiffness are presented in figure 11. This figure shows the results of models with the same area fraction of pillars ($\beta_1 = 2.0\%$) and asperities ($\beta_2 = 40.0\%$). The figures clearly indicate that Young's modulus of the organic matrix affects the early stages of deformation just before the sliding step starts. An increase in Young's modulus of the organic matrix results in an increase in Young's modulus of the multilayered material. Our results also show that the stiffness of the organic matrix has a marginal effect on the ultimate strength of the models.

To investigate the effect of area fraction of asperities (effective organic matrix) on the system, two models with similar material properties of the organic matrix, mineral platelets and pillars, and similar pillars' area fraction and platelets' aspect ratio ($L/D = 8.0$) with different area fraction of asperities (β_2) were constructed. The results in figure 12 show that the model with lower area fraction of asperities has lower strength.

To study the role of pillars, models with different area fraction of pillars varying from $\beta_1 = 1.0$ to 4.0% were developed. Figure 13 shows the effect of pillars in models for an organic matrix with stiffness value of ($E_m = 4.0$ GPa) and asperities' area fraction of ($\beta_2 = 40.0\%$). The results show that initial stiffness of the material is the same for all models. However, the ultimate strength and ductility increases slightly as area fraction of the pillars increases. Hence, different area fraction of pillars leads to different tensile toughness.

4. Discussion

4.1. Unit-cell behaviour and nacre micromechanical model

The unit-cell response helps us to understand how geometry and mechanics affect different mechanical properties of nacre by multiple breakages of the links between the platelets. Figure 5*a* shows the result of the unit-cell model simulation. Initially, all the components carry the load until the organic matrix in both layers, which are in series with the platelets,

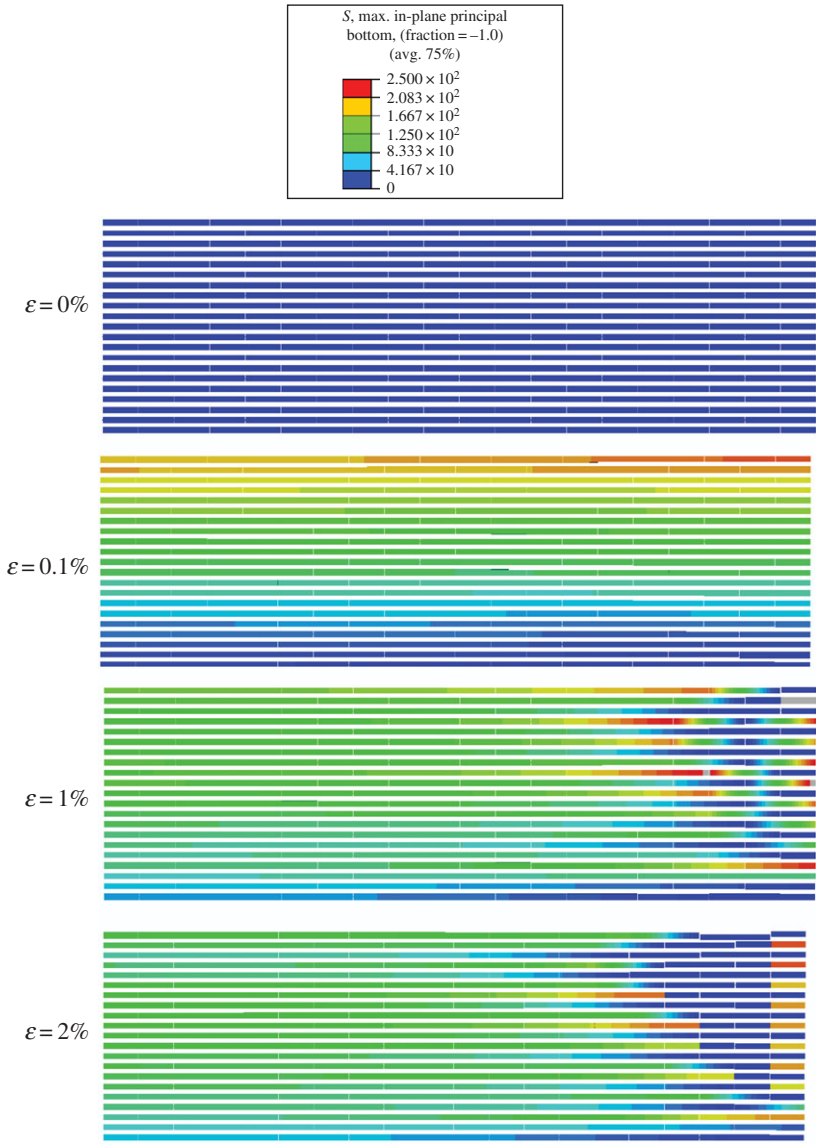

Figure 9. Maximum in-plane principal stress distribution for a model in four steps of simulation.

fail. Later, the load is carried by the pillars and the proteins in shear until the pillars, the more brittle components break. Finally, the proteins in shear are the only components that carry the entire load.

The numerical result of the suggested micromechanical super-cell model clearly shows the ability of the model to predict the experimental results on a multilayered biological material (nacre). Young's modulus, the large inelastic deformation, the ultimate strength and the tensile toughness fits well with the experimental data [23,57]. Each drop in the stress–strain graph of the nacre-like structure shows the brittle breaking of a link in the system. Hence, the stress–strain curve of real nacre, which contains several thousands of platelets in several thousands of layers, is made by gradual failure of millions of links.

There are different analytical solutions to estimate the stiffness of the multilayered structure [64]. One of these solutions is Riley's model [65]:

$$E_{\text{nacre}} = V_{\text{p}}E_{\text{p}}\left(1 - \frac{\log \delta}{\delta}\right) + (1 - V_{\text{p}})E_{\text{m}}, \tag{4.1}$$

where

$$\delta = s\sqrt{\frac{G_{\text{m}}V_{\text{p}}}{E_{\text{p}}(1 - V_{\text{p}})}}, \tag{4.2}$$

where s is the platelet aspect ratio; E_{p}, E_{m} and E_{nacre} are Young's moduli of the platelets, the organic matrix and nacre, respectively. G_{m} is the shear modulus of the organic matrix and V_{p} is the volume concentration of mineral. Gao presented another solution to find the stiffness of the composite [66]

$$\frac{1}{E_{\text{nacre}}} = \frac{4(1 - V_{\text{p}})}{G_{\text{m}}V_{\text{p}}{}^2 s^2} + \frac{1}{V_{\text{p}}E_{\text{p}}}, \tag{4.3}$$

where E_{p} is Young's modulus of the platelets, G_{m} is the shear modulus of the organic matrix, V_{p} is the volume concentration of mineral and s is the aspect ratio of the mineral platelets.

Equations (4.1) and (4.3) provide similar solutions for the numbers considered here. Therefore, using equation (3.3), the stiffness of the multilayered system can be estimated

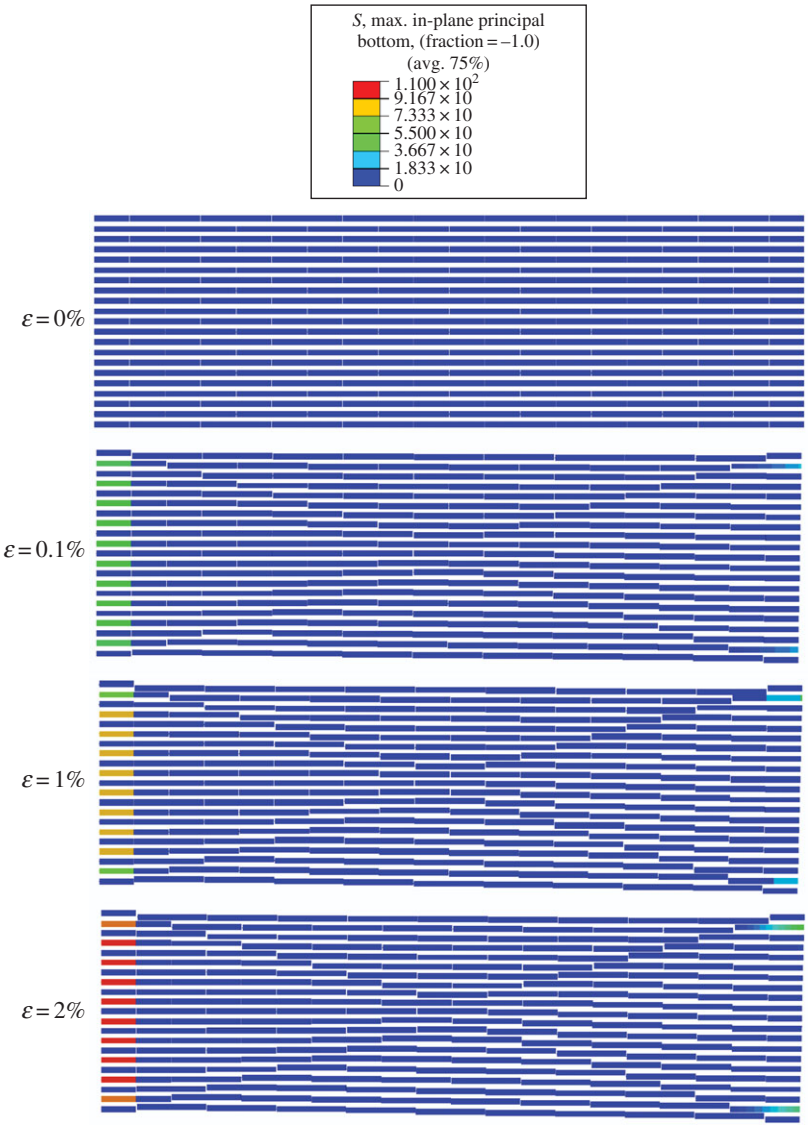

Figure 10. Maximum in-plane principal stress distribution for a model consisting of only pillars and asperities, in four steps of simulation.

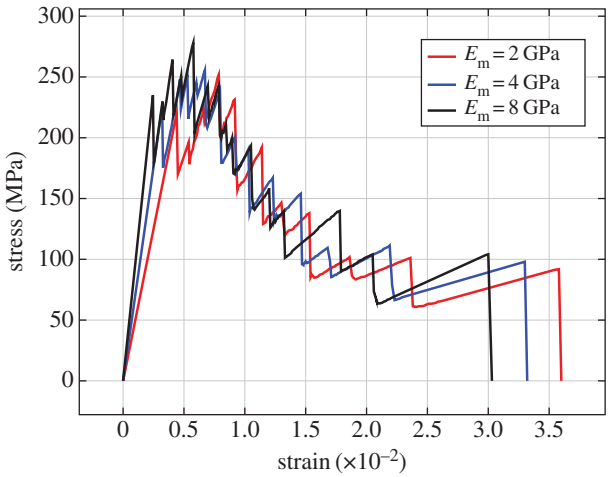

Figure 11. Stress–strain plots for $L/D = 16.0$ and different values of the organic matrix stiffness (E_m). (Online version in colour.)

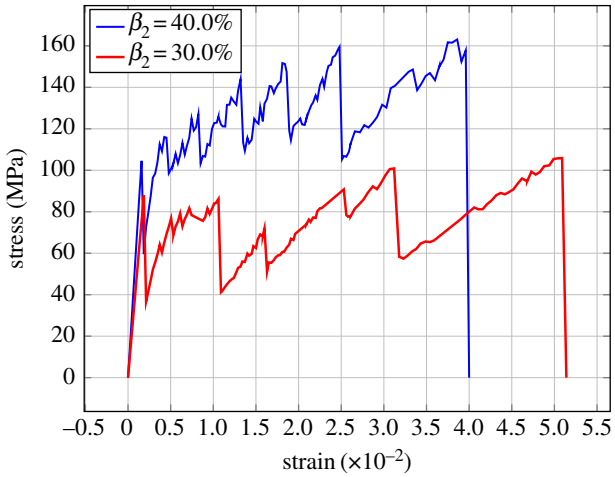

Figure 12. Stress–strain plots for models with $E_m = 4.0$ GPa and $L/D = 8.0$. (Online version in colour.)

as $E = 64.3$ GPa which is in agreement with the simulation result ($E = 65.4$ GPa).

Another analytical solution for brick and mortar structure, proposed by Begley *et al.* [60], shows the stiffness to be about 75 GPa for the modelled structure. In this analytical solution, the mortar stiffness is approximated as

$$\frac{E_m}{fE_p} \sim 0.8, \tag{4.4}$$

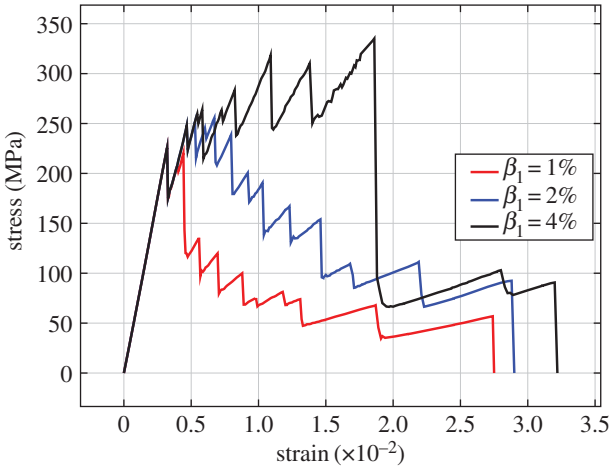

Figure 13. Stress–strain curves for models with $L/D = 16.0$ and three different values of β_1. (Online version in colour.)

where f is the volume fraction of the mortar phase, E_m is the elastic modulus of the mortar and E_p is the elastic modulus of the bricks. Hence, the composite modulus ratio (E_c/E_p) (E_c is Young's modulus of composite) would be around 0.75 for the platelets' aspect ratio of $L/D = 8.0$.

4.2. Toughening mechanism and the role of the components

Figure 7 shows the effect of an important factor in nacre-like materials, which is the platelets' aspect ratio, L/D. The results show that the aspect ratio of platelets affects the stiffness of the material. For $L/D = 5.0$ and 6.0, the stiffness is calculated to be about $E = 53.5$ GPa and $E = 59.6$ GPa, respectively. By increasing the aspect ratio to $L/D = 8.0$, which is close to aspect ratio of nacre, the stiffness rises to $E = 65.4$ GPa. The stiffnesses of the models with aspect ratio of 10.0, 12.0 and 16.0 are 71.5 GPa, 78.1 GPa and 80.3 GPa, respectively. These results also show that the overall tensile toughness and strength of the multilayered material is a function of the platelets' aspect ratio. These computed stiffness values agree well with the analytical results obtained by equation (4.3). This agreement also shows that the low area fraction of the pillar does not affect the stiffness of the multilayered materials. The results are summarized in table 1.

The volume concentration of mineral will decrease as the platelets' aspect ratio increases in the simulations. Hence, the volume concentrations (ϕ) for the models with aspect ratio of 5.0, 6.0, 8.0, 10.0, 12.0 and 16.0 are approximately 96.7%, 96.3%, 95.8%, 95.4%, 95.0% and 93.8%, respectively. Additionally, as it is shown in figure 7*b*, the optimum platelets' aspect ratio for the highest tensile toughness is cot $L/D = 12.0$. This result is higher than the model by Gao *et al.* [51], where the optimum aspect ratio of the mineral platelets, s^*, can be computed as

$$s^* = \frac{1}{\tau_m^f}\sqrt{\frac{\pi E_p \gamma}{h}}, \tag{4.5}$$

where τ_m^f is the shear strength of the organic matrix, E_p is Young's modulus of platelets, γ is the surface energy (assumed to be 1 J m^{-2}) and h is the thickness of mineral crystal. This equation results in an aspect ratio of $s^* = 10$ ($L/D = 10$). The difference between our model and this model can be attributed to the existence of pillars and asperities in the presented model.

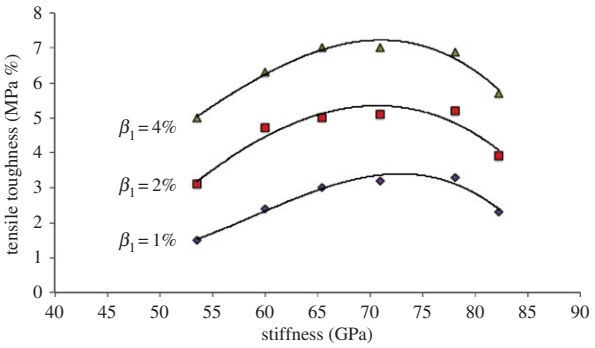

Figure 14. Effects of the area fraction of pillars on the tensile toughness of the bioinspired multilayered materials. (Online version in colour.)

Table 1. The effect of the platelets' aspect ratio on the stiffness.

platelets' aspect ratio	analytical solution (GPa) equation (4.3)	simulation results (GPa)
5.0	52.2	53.5
6.0	57.8	59.6
8.0	65.9	65.4
10.0	73.1	71.5
12.0	77.3	78.1
16.0	80.7	80.3

The effects of area fraction of pillars on the optimum tensile toughness of the models is presented in figure 14. The plot clearly shows an optimum value of tensile toughness for a constant area fraction of the pillars as a function of platelets' aspect ratio. The graphs also show that increasing the area fraction of pillars results in a slight decrease in the stiffness corresponding to the highest tensile toughness. It must be noted that, physically, the area fraction of pillars cannot be increased to a large number since they need to remain at nanoscale in the structure. Moreover, a large increase in the area fraction of pillars causes the fracture of platelets, which significantly decreases the tensile toughness of the multilayered system.

The trend in the increase of the ultimate strength of the models as a function of platelet aspect ratio is also in agreement with previous analytical solutions. Analytical solutions for a brick and mortar structure show that samples with higher platelets' aspect ratios generally have higher strength [60].

To investigate the effect of Young's modulus of the organic matrix, three models with similar platelets' aspect ratios ($L/D = 16.0$), similar area fraction of pillars ($\beta_1 = 2.0\%$), similar area fraction of asperities ($\beta_2 = 40.0\%$) and with three different values for the stiffness of the organic matrix were constructed. The results are summarized in table 2. Higher values of Young's modulus for the organic matrix result in higher stiffness of the model. The ultimate strength and the breaking strain for all the models are similar. Hence, the stiffness of the organic layer significantly contributes to the stiffness of multilayered material. These results match the results of the analytical solution in equation (4.3). Furthermore, these results are similar to the experimental

Table 2. The effect of Young's modulus of the organic matrix on the stiffness of the models.

Young's modulus of proteins (GPa)	analytical solution (GPa) equation (4.3)	simulation results (GPa)
2.0	70.9	68.0
4.0	80.7	80.3
8.0	86.8	86.6

results on wet and dry nacre. Dry nacre shows higher stiffness and higher strength but lower ductility [1]. The results show that drying the shell will make the organic matrix stiffer, so that nacre would be stiffer; however, the ductility and toughness would significantly decrease.

As it was mentioned earlier, the role of asperities is to confine the proteins to the proximity of minerals and enhance the organic–inorganic interactions. Hence, in the presented model, the area fraction of asperities (effective organic matrix) has the same effect as Young's modulus of the organic matrix. In other words, the area fraction of asperities essentially controls the role of the organic matrix in the system. The results in figure 12 present this effect in the overall mechanical behaviour of the system.

To explore the role of pillars in the system, the ultimate strength for the models is obtained, and the results are summarized in table 3. This clearly shows that higher area fraction of pillars results in higher ultimate strength of the multilayered material. Figure 13 also shows that the models with higher area fraction of pillars have higher inelastic deformation. Analytical studies by Begley *et al.* [60] on a brick and mortar structure show that increasing the mortar strength will increase the ultimate strength of the material [60]. Increasing the area fraction of shear pillars has a similar effect on ultimate strength, as strengthening the mortar part in brick and mortar structure, which causes higher strength for the multilayered materials with a similar aspect ratio of platelets.

5. Conclusion

Brittleness is the main deficiency of ceramics and tremendous efforts have been made to overcome it. Although abalone nacre is mostly made of a ceramic, it is strong and super-tough. This study presented a simple mechanics-based model for exploring the mechanical properties of nacre and similar multilayered materials. Stiffness, strength and inelastic deformation of the suggested model are in excellent agreement with the available experimental data on abalone nacre.

Table 3. The effect of area fraction of pillars on the ultimate strength.

area fraction of pillars (%)	simulation results (MPa)
1.0	225
2.0	260
4.0	340

The overall performance of multilayered bioinspired materials depends on four important factors: aspect ratio of platelets, (shear) pillars, organic matrix and asperities. A mechanics-based model was developed by addition of the nanoscale pillars and assuming a realistic stiffness value for the organic matrix that can accurately simulate the mechanical behaviour of abalone nacre. The results show that the aragonite platelets, pillars and the organic matrix synergistically affect the stiffness of nacre. The results also show that pillars play an important role in the strength and tensile toughness of abalone nacre through two mechanisms (i) directly, by inclusion of their own stiffness and strength and (ii) indirectly, by stiffening the organic matrix. The highly nonlinear behaviour of the suggested multilayered material is a result of a distributed deformation in the nacre-like structure due to existence of nanoscale features with near theoretical strength. The distributed deformation mechanism is proposed as the main toughening mechanism in the biological multilayered material. Hence, it is essential to understand that the superb mechanical properties of nacre are a direct result of optimal geometry, existence of nanoscale elements such as pillars and asperities, and an organic matrix with outstanding mechanical properties.

Acknowledgement. We are grateful to Dr I. A. Aksay and J. H. Prevost for insightful discussions.

Funding statement. We are truly grateful to support from NSF CAREER grant no. 1261284.

Endnote

[1]In this paper, *tensile toughness* is defined as area under the stress–strain curve.

References

1. Jackson AP, Vincent JFV, Turner RM. 1988 The mechanical design of nacre. *Proc. R. Soc. Lond. B* **234**, 415–440. (doi:10.1098/rspb.1988.0056)
2. Meyers MA, Chen PY, Lin AYM, Seki Y. 2008 Biological materials: structure and mechanical properties. *Prog. Mater. Sci.* **53**, 1–206. (doi:10.1016/j.pmatsci.2007.05.002)
3. Espinosa HD, Rim JE, Barthelat F, Buehler MJ. 2009 Merger of structure and material in nacre and bone: perspectives on de novo biomimetic materials. *Prog. Mater. Sci.* **54**, 1059–1100. (doi:10.1016/j.pmatsci.2009.05.001)
4. Meyers MA, McKittrick J, Chen PY. 2013 Structural biological materials: critical mechanics–materials connections. *Science* **339**, 773–779. (doi:10.1126/science.1220854)
5. Porter MM *et al.* 2012 Magnetic freeze casting inspired by nature. *Mater. Sci. Eng. A.* **556**, 741–750. (doi:10.1016/j.msea.2012.07.058)
6. Munch E, Launey ME, Alsem DH, Saiz E, Tomsia AP, Ritchie RO. 2008 Tough, bio-inspired hybrid materials. *Science* **322**, 1516–1520. (doi:10.1126/science.1164865)
7. Mohanty B, Katti KS, Katti DR. 2008 Experimental investigation of nanomechanics of the mineral-protein interface in nacre. *Mech. Res. Commun.* **35**, 17–23. (doi:10.1016/j.mechrescom.2007.09.006)
8. Launey ME, Munch E, Alsem DH, Saiz E, Tomsia AP, Ritchie RO. 2010 A novel biomimetic approach to the design of high-performance ceramic/metal composites. *J. R. Soc. Interface* **7**, 741–753. (doi:10.1098/rsif.2009.0331)

9. Wang RZ, Wen HB, Cui FZ, Zhang HB, Li HD. 1995 Observations of damage morphologies in nacre during deformation and fracture. *J. Mater. Sci.* **30**, 2299–2304. (doi:10.1007/BF01184577)
10. Ritchie RO. 2011 The conflicts between strength and toughness. *Nat. Mater.* **10**, 817–822. (doi:10.1038/nmat3115)
11. Ortiz C, Boyce MC. 2008 Bioinspired structural materials. *Science* **319**, 1053–1054. (doi:10.1126/science.1154295)
12. Hunger PM, Donius AE, Wegst UG. 2013 Platelets self-assemble into porous nacre during freeze casting. *J. Mech. Behav. Biomed. Mater.* **19**, 87–93. (doi:10.1016/j.jmbbm.2012.10.013)
13. Bonderer LJ, Feldman K, Gauckler LJ. 2010 Platelet-reinforced polymer matrix composites by combined gel-casting and hot-pressing. Part I: Polypropylene matrix composites. *Compos. Sci. Technol.* **70**, 1958–1965. (doi:10.1016/j.compscitech.2010.07.014)
14. Tang Z, Kotov NA, Magono S, Ozturk B. 2003 Nanostructured artificial nacre. *Nat. Mater.* **2**, 413–418. (doi:10.1038/nmat906)
15. Bouville F, Maire E, Meille S, Van de Moortle B, Stevenson AJ, Deville S. 2014 Strong, tough and stiff bioinspired ceramics from brittle constituents. *Nat. Mater.* **13**, 508–514. (doi:10.1038/nmat3915)
16. Ji B, Gao H. 2004 Mechanical properties of nanostructured biological materials. *J. Mech. Phys. Solids* **52**, 1963–1990.
17. Jackson AP, Vincent JFV, Turner RM. 1989 A physical model of nacre. *Compos. Sci. Technol.* **36**, 255–266. (doi:10.1016/0266-3538(89)90024-9)
18. Bass JD. 1995 Elasticity of minerals, glasses, and melts. In *Mineral physics & crystallography: a handbook of physical constants* (ed. TJ Ahrens), pp. 45–63. Washington, DC: American Geophysical Union.
19. Currey JD, Taylor JD. 1974 The mechanical behavior of some molluscan hard tissues. *J. Zool. Lond.* **173**, 395–406. (doi:10.1111/j.1469-7998.1974.tb04122.x)
20. Currey JD. 1976 Further studies on the mechanical properties of mollusc shell material. *J. Zool. Lond.* **180**, 445–453. (doi:10.1111/j.1469-7998.1976.tb04690.x)
21. Verma D, Katti K, Katti D. 2007 Nature of water in nacre: a 2D Fourier transform infrared spectroscopic study. *Spectrochim. Acta A* **67**, 784–788. (doi:10.1016/j.saa.2006.08.033)
22. Mohanty B, Katti KS, Katti DR, Verma D. 2006 Dynamic nanomechanical response of nacre. *J. Mater. Res.* **21**, 2045–2051. (doi:10.1557/jmr.2006.0247)
23. Wang RZ, Suo Z, Evans AG, Yao N, Aksay IA. 2001 Deformation mechanism in nacre. *J. Mater. Res.* **16**, 2485–2493. (doi:10.1557/JMR.2001.0340)
24. Feng QL, Cui FZ, Pu G, Wang RZ, Li HD. 2000 Crystal orientation, toughening mechanisms and a mimic of nacre. *Mater. Sci. Eng. C.* **11**, 19–25. (doi:10.1016/S0928-4931(00)00138-7)
25. Barthelat F, Espinosa HD. 2007 An experimental investigation of deformation and fracture of nacre/mother of pearl. *Exp. Mech.* **47**, 311–324. (doi:10.1007/s11340-007-9040-1)
26. Barthelat F, Li CM, Comi C, Espinosa HD. 2006 Mechanical properties of nacre constituents and their impact on mechanical performance. *J. Mater. Res.* **21**, 1977–1986. (doi:10.1557/jmr.2006.0239)
27. Li X, Chang WC, Chao YJ, Wang R, Chang M. 2004 Nanoscale structural and mechanical characterization of a natural nanocomposite material: the shell of red abalone. *Nano Lett.* **4**, 613–617. (doi:10.1021/nl049962k)
28. Bruet BJ F, Qi HJ, Boyce MC, Panas R, Tai K, Frick L, Ortiz C. 2005 Nanoscale morphology and indentation of individual nacre tablets from the gastropod mollusc *Trochus niloticus*. *J. Mater. Res.* **20**, 2400–2419. (doi:10.1557/jmr.2005.0273)
29. Smith BL, Schaffer TE, Viani M, Thompson JB, Frederick NA, Kindt J, Hansma PK. 1999 Molecular mechanistic origin of the toughness of natural adhesives, fibres and composites. *Nature* **399**, 761–763. (doi:10.1038/21607)
30. Katti KS, Mohanty B, Katti DR. 2006 Nanomechanical properties of nacre. *J. Mater. Res.* **21**, 1237–1242. (doi:10.1557/jmr.2006.0147)
31. Moshe-Drezner H, Shilo D, Dorogoy A, Zolotoyabko E. 2010 Nanometer-scale mapping of elastic modules in biogenic composites: the nacre of mollusk shells. *Adv. Funct. Mater.* **20**, 2723–2728. (doi:10.1002/adfm.200902165)
32. Xu ZH, Yang Y, Huang Z, Li X. 2011 Elastic modulus of biopolymer matrix in nacre measured using coupled atomic force microscopy bending and inverse finite element techniques. *Mater. Sci. Eng. C.* **31**, 1852–1856. (doi:10.1016/j.msec.2011.08.023)
33. Stempfle P, Pantale O, Njiwa RK, Rousseau M, Lopez E, Bourrat X. 2007 Friction-induced sheet nacre fracture: effects of nano-shocks on cracks location. *Int. J. Nanotechnol.* **4**, 712–729.
34. Stempfle PH, Pantale O, Rousseau M, Lopez E, Bourrat X. 2010 Mechanical properties of the elemental nanocomponents of nacre structure. *Mater. Sci. Eng. C.* **30**, 715–721. (doi:10.1016/j.msec.2010.03.003)
35. Ghosh P, Katti DR, Katti KS. 2007 Mineral proximity influences mechanical response of proteins in biological mineral-protein hybrid systems. *Biomacromolecules* **8**, 851–856. (doi:10.1021/bm060942h)
36. Xu ZH, Li X. 2011 Deformation strengthening of biopolymer in nacre. *Adv. Funct. Mater.* **21**, 3883–3888. (doi:10.1002/adfm.201100167)
37. Schaffer TE, Ionescu-Zanetti C, Proksch R, Fritz M, Walters DA, Almqvist N, Hansma PK. 1997 Does abalone nacre form by heteroepitaxial nucleation or by growth through mineral bridges? *Chem. Mater.* **9**, 1731–1740. (doi:10.1021/cm960429i)
38. Meyers MA, Lin AYM, Chen PY, Muyco J. 2008 Mechanical strength of abalone nacre: role of the soft organic layer. *J. Mech. Behav. Biomed. Mater.* **1**, 76–85. (doi:10.1016/j.jmbbm.2007.03.001)
39. Weiner S, Lowenstam H. 1986 Organization of extracellularly mineralized tissues: a comparative study of biological crystal growth. *Cr. Rev. Biochem. Mol. Biol.* **20**, 365–408. (doi:10.3109/10409238609081998)
40. Addadi L, Weiner S. 1997 Biomineralization: a pavement of pearl. *Nature* **389**, 912–915. (doi:10.1038/40010)
41. Song F, Soh AK, Bai YL. 2003 Effect of nanostructures on the fracture strength of the interfaces in nacre. *J. Mater. Res. Soc.* **18**, 8. (doi:10.1557/JMR.2003.0003)
42. Song F, Soh AK, Bai YL. 2003 Structural and mechanical properties of the organic matrix layers of nacre. *Biomaterials* **24**, 3623–3631. (doi:10.1016/S0142-9612(03)00215-1)
43. Cartwright JH, Checa AG. 2007 The dynamics of nacre self-assembly. *J. R. Soc. Interface* **4**, 491–504. (doi:10.1098/rsif.2006.0188)
44. Hou WT, Feng QL. 2003 Crystal orientation preference and formation mechanism of nacreous layer in mussel. *J. Cryst. Growth.* **258**, 402–408. (doi:10.1016/S0022-0248(03)01551-3)
45. Checa AG, Rodrguez-Navarro AB. 2005 Self-organisation of nacre in the shells of Pterioida (Bivalvia: Mollusca). *Biomaterials* **26**, 1071–1079. (doi:10.1016/j.biomaterials.2004.04.007)
46. Checa AG, Okamoto T, Ramrez J. 2006 Organization pattern of nacre in Pteriidae (Bivalvia: Mollusca) explained by crystal competition. *Proc. R. Soc. B* **273**, 1329–1337. (doi:10.1098/rspb.2005.3460)
47. Checa AG, Cartwright JH, Willinger MG. 2011 Mineral bridges in nacre. *J. Struct. Biol.* **176**, 330–339. (doi:10.1016/j.jsb.2011.09.011)
48. Dimas LS, Bratzel GH, Eylon I, Buehler MJ. 2013 Tough composites inspired by mineralized natural materials: computation, 3D printing, and testing. *Adv. Func. Mater.* **23**, 4629–4638. (doi:10.1002/adfm.201300215)
49. Dimas LS, Buehler MJ. 2014 Modeling and additive manufacturing of bio-inspired composites with tunable fracture mechanical properties. *Soft Matter.* **10**, 4436–4442. (doi:10.1039/c3sm52890a)
50. Currey JD. 1977 Mechanical properties of mother of pearl in tension. *Proc. R. Soc. Lond. B* **196**, 443–463. (doi:10.1098/rspb.1977.0050)
51. Gao H, Ji BH, Jager IL, Arzt E, Fratzl P. 2003 Materials become insensitive to flaws at nanoscale: Lessons from nature. Proc. Natl Acad. Sci. *USA* **100**, 5597–5600. (doi:10.1073/pnas.0631609100)
52. Katti DR, Katti KS, Sopp JM, Sarikaya M. 2001 3D finite element modeling of mechanical response in nacre-based hybrid nanocomposites. *Comput. Theor. Polym. Sci.* **11**, 397–404. (doi:10.1016/S1089-3156(01)00012-5)
53. Katti KS, Katti DR, Pradhan SM, Bhosle A. 2005 Platelet interlocks are the key to toughness and strength in nacre. *J. Mater. Res.* **20**, 1097–1100. (doi:10.1557/JMR.2005.0171)
54. Sen D, Buehler MJ. 2011 Structural hierarchies define toughness and defect-tolerance despite simple and mechanically inferior brittle

building blocks. *Sci. Rep.* **1**, 35. (doi:10.1038/srep00035)

55. Katti DR, Katti KS. 2001 Modeling microarchitecture and mechanical behavior of nacre using 3D finite element techniques. *J. Mater. Sci.* **36**, 1411–1417. (doi:10.1023/A:1017528209162)
56. Katti DR, Pradhan SM, Katti KS. 2004 Modeling the organic–inorganic interfacial nanoasperities in a model bio-nanocomposite, nacre. *Rev. Adv. Mater. Sci.* **6**, 162–168.
57. Evans AG, Suo Z, Wang RZ, Aksay IA, He MY, Hutchinson JW. 2001 Model for the robust mechanical behavior of nacre. *J. Mater. Res.* **16**, 2475–2484. (doi:10.1557/JMR.2001.0339)
58. Shao Y, Zhao HP, Feng XQ, Gao H. 2012 Discontinuous crack-bridging model for fracture toughness analysis of nacre. *J. Mech. Phys. Solids* **60**, 1400–1419. (doi:10.1016/j.jmps.2012.04.011)
59. Shao Y, Zhao HP, Feng XQ. 2014 On flaw tolerance of nacre: a theoretical study. *J. R. Soc. Interface* **11**, 20131016. (doi:10.1098/rsif.2013.1016)
60. Begley MR, Philips NR, Compton BG, Wilbrink DV, Ritchie RO, Utz M. 2012 Micromechanical models to guide the development of synthetic 'brick and mortar' composites. *J. Mech. Phys. Solids* **60**, 1545–1560. (doi:10.1016/j.jmps.2012.03.002)
61. Rabiei R, Bekah S, Barthelat F. 2010 Failure mode transition in nacre and bone-like materials. *Acta Biomater.* **6**, 4081–4089. (doi:10.1016/j.actbio.2010.04.008)
62. Neves NM, Mano JF. 2005 Structure/mechanical behavior relationships in crossed-lamellar sea shells. *Mater. Sci. Eng. C.* **25**, 113–118. (doi:10.1016/j.msec.2005.01.004)
63. Dimas LS, Buehler MJ. 2012 Influence of geometry on mechanical properties of bio-inspired silica-based hierarchical materials. *Bioinspir. Biomim.* **7**, 036024. (doi:10.1088/1748-3182/7/3/036024)
64. Barthelat F, Rabiei R. 2011 Toughness amplification in natural composites. *J. Mech. Phys. Solids* **59**, 829–840. (doi:10.1016/j.jmps.2011.01.001)
65. Lusis J, Woodhams RT, Xanthos M. 1973 The effect of flake aspect ratio on the flexural properties of mica reinforced plastics. *Polym. Eng. Sci.* **13**, 139–145. (doi:10.1002/pen.760130210)
66. Jager I, Fratzl P. 2000 Mineralized collagen fibrils: a mechanical model with a staggered arrangement of mineral particles. *Biophys. J.* **79**, 1737–1746. (doi:10.1016/S0006-3495(00)76426-5)